

Article

Monitoring and Analysing Changes in Temperature and Energy in the Ground with Installed Horizontal Ground Heat Exchangers

Pavel Pauli, Pavel Neuberger * and Radomír Adamovský

Department of Mechanical Engineering, Faculty of Engineering, Czech University of Life Sciences Prague, Kamýčká 129, Prague-Suchbát 165 21, Czech Republic; paulip@tf.czu.cz (P.P.); adamovsky@tf.czu.cz (R.A.)

* Correspondence: neuberger@tf.czu.cz; Tel.: +420-224-383-179; Fax: +420-234-381-828

Academic Editor: Vincent Lemort

Received: 10 May 2016; Accepted: 1 July 2016; Published: 28 July 2016

Abstract: The objective of this work was to monitor and analyse temperature changes in the ground with installed linear and Slinky-type horizontal ground heat exchangers (HGHEs), used as low-potential heat pump energy sources. Specific heat flows and specific energies extracted from the ground during the heating season were also measured and compared. The verification results showed that the average daily ground temperatures with the two HGHEs are primarily affected by the temperature of the ambient environment. The ground temperatures were higher than ambient temperature during most of the heating season, were only seldom below zero, and were higher by an average 1.97 ± 0.77 K in the ground with the linear HGHE than in the ground with the Slinky-type HGHE. Additionally, the specific thermal output extracted from the ground by the HGHE was higher by 8.45 ± 16.57 W/m² with the linear system than with the Slinky system. The specific energies extracted from the ground over the whole heating season were 110.15 kWh/m² and 57.85 kWh/m² for the linear and Slinky-type HGHEs, respectively.

Keywords: ground; ground source heat pumps systems; heat pump; horizontal ground heat exchangers; specific heat flows; specific energies; temperatures

1. Introduction

According to the Intergovernmental Panel on Climate Change report [1], CO₂ emissions should decrease by 40%–70% during the 2010–2050 period and global temperature increase should be limited by 2 °C compared to the level existing before the industrial revolution. The use of heat pumps for room heating and water heating may significantly help reach those ambitious targets. Statistical information of the U.S. Energy Information Administration, Residential Energy Consumption Survey (RECS) [2] shows that the share of energy use in residential and commercial buildings in total energy use in the country exceeds 22%. In this, about 65% energy is spent on room heating, residential house cooling, and hot water heating. Previous research [3] suggested that power systems with heat pumps consume 42%–62% less energy than the conventional heating/cooling systems. In contrast to other renewable sources (solar energy, wind energy), heat pumps transform energy directly between the low-potential energy source and the building without any need for additional heat transfer or accumulation.

Natural low-potential energy sources for heat pumps include air, surface water or groundwater, and ground or rock masses. According to the EHPA statistical report [4], the heat pumps predominating before 2006 were the ground-water type, whereas the air-water type started to predominate after that date. Currently, 61.07% of the installed heat pumps are the air-water type, 33.97% are the ground-water type, 2.84% are the water-water type, and 2.12% use other sources. The air-water pump type seems to owe its large-scale use to the lower investment costs and simple design. The energy savings and the operating costs, however, are not that beneficial.

In a reversed Carnot cooling cycle, the effect, which is expressed by the heating factor for a heat pump, is higher the smaller the temperature difference is between the cycle heat input and output. Assuming a constant condensation temperature, a higher heating factor can be attained via a higher evaporation temperature. The results of practical testing [5–7], as well as modelling [8], have shown that the ground temperatures are higher than the ambient temperatures during the major part of the heating season, whereas the reverse is true during the summer season. Hence, the ground is a convenient, stable, low-potential heat pump source for building heating in winter and for their cooling in summer.

The low-potential heat is extracted from/delivered to the rock/ground by means of vertical ground heat exchangers (VGHEs) or horizontal ground heat exchangers (HGHEs). VGHEs require a minimal land plot area, they work at a high efficiency, and are considered to be among the most stable low-potential energy sources; their installation, however, is very costly. HGHEs, existing in three design variants—linear, helical, or spiral [9], require a larger land area but are less costly. They are a compromise between a high efficiency and the investment costs. Petit and Meyer [10] examined the power and financial parameters of heat pumps using the following low-potential sources: air, HGHEs, and VGHEs. Air, as an energy source for heat pumps, emerged as the poorest of them. VGHEs provided the highest power output and HGHEs exhibited the most convenient heating factor and financial parameters. De Swart and Meyer [11] reported that at low ambient temperatures, the ground-water heat pump type provides a heating power and a heating factor 24% and 20%, respectively, higher than the air-water heat pump type.

Our measurements were aimed to:

- Analyse temperature changes in the ground with a linear HGHE and a Slinky-type exchanger during the heating season;
- Assess the effect of the HGHE configuration on the temperature values and distribution in the ground;
- Assess the effect of the HGHE configuration on the specific heat flows and specific energies extracted from the ground.

The following hypotheses were tested:

- (a) The ground temperatures will be largely above zero during the heating season for both exchanger types. The ground temperatures in the exchanger area will be rarely below zero;
- (b) The temperatures of the ground with the linear HGHE will be higher than those with the Slinky-type exchanger;
- (c) The specific heat flows and specific energies extracted from the ground by the HGHE will be higher for the linear HGHE type than for the Slinky type.

The temperature distribution across the ground, the temperature gradients, and the heat flow densities shared between the ground surface and the surrounding environment were investigated by Popiel et al. [12]. Heat energy extraction from the ground, specific heat output of a linear HGHE and a Slinky-type HGHE, and the effect of the incident solar radiation on the ground energy balance were studied in detail by Wu et al. [13]. Garcia et al. [14] examined the interaction between the ground and an HGHE and found that heat extraction by the HGHE had a pronounced effect not only on the temperature, but also on the moisture, of the ground. The importance of knowledge of the ground temperature and of the climatic data of the ambient environment and their changes throughout the year, with respect to the HGHE configuration design, is stressed in the publication by Hepburn et al. [15], who examined the power and sustainability of HGHEs as low-potential energy sources for heat pumps depending on the ground temperatures and heat parameters. Extensive measurements resulted in a deeper insight into the effects of heat extraction by an HGHE and of the climatic conditions on the ground temperatures. Sanaye and Niroomand [16] engaged themselves in design optimisation and use

of different configurations of linear HGHEs in relation to the ground temperature, extracted energy flows, and use of ground source heat pump (GSHP) systems, while Wu et al. [13] examined the design and operation of Slinky-type HGHEs with respect to similar parameters and conditions. Zarrella and De Carli [17] paid thorough attention to the impact of the interaction between the ground surface and environment on the performance of HGHE and on the effect of the heat pump. They created a model of thermal resistances and capacities respecting the state of the environment, solar radiation intensity, heat transfer via the radiation of the Earth's surface to the sky, and the influence of the spacing of tubes of a spiral heat exchanger. They analysed the model in detail and verified it in operational mode. The simulation results showed good agreement with measurements and also showed an insignificant effect of the spacing of tubes of a spiral heat exchanger.

Requirements for the ground temperature with respect to the temperature of the HGHE's heat-transfer fluid are set by the German VDI standard [18]. The effects of the ground moisture on the HGHE heat output and on the COP were investigated by Leong et al. [19]. Wu et al. [20] examined the temperatures of the ground with HGHEs used as low-potential energy sources for a conventional heat pump with a compressor and for an absorption type heat pump. The factors that affect the important thermal conductivity coefficient of the ground were analysed by Song et al. [21] and by Banks [22]. The effect of rainfall on the ground heat parameters and on the HGHE power was in the focus of Go et al. [23].

2. Materials and Methods

2.1. Measurement Methods

The linear horizontal ground heat exchanger was manufactured from polyethylene piping PE 100RC 40 mm × 3.7 mm (LUNA PLAST a. s., Hořín, Czech Republic), resistant to point loads and to the occurrence of cracks. The heat exchanger piping with the total length of 330 m (41.473 m²) was installed at a depth of 1.8 m in 3 loops at a 1 m span. The length of each loop was 54.62 m. Layouts of the HGHE and the locations of the temperature sensors are shown in Figures 1 and 2.

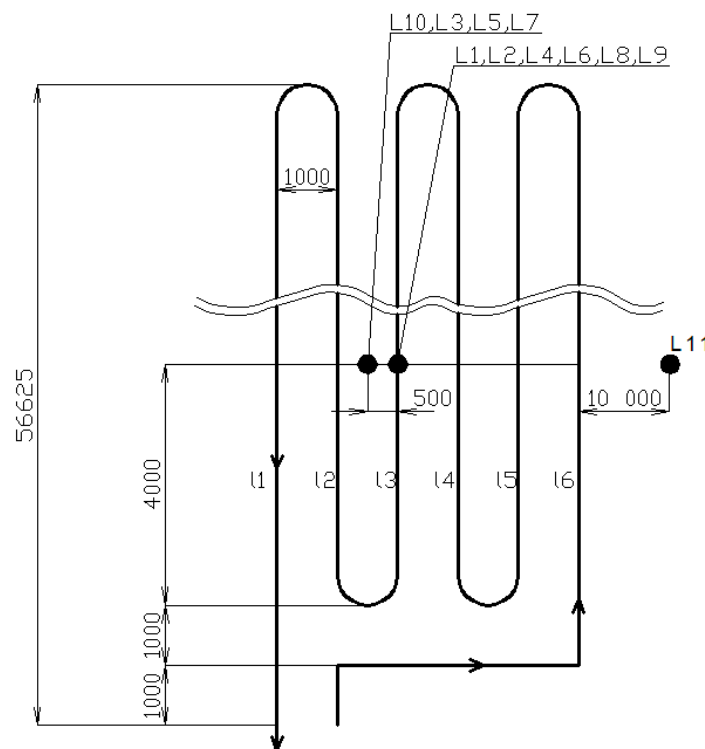


Figure 1. Ground layout of the linear HGHE and locations of the temperature sensors (Unit: mm).

- t_{GR} = ground temperature ($^{\circ}\text{C}$)
 \bar{t}_G = mean ground temperature ($^{\circ}\text{C}$)
 Δt_A = oscillation amplitude around the temperature \bar{t}_G (K)
 τ = number of days from the start of measurement (day)
 φ = initial phase of oscillation (rad)
 Ω = angular velocity ($2\pi/365$ rad/day)

This equation expresses nonlinear regression of y on x , and so the degree of tightness between the two parameters was characterized by the determination index I_{yx}^2 (Bowerman et al. [26]). Equation (1) expresses only the course of the ground temperature in the HGHE area during the heating season. It does not aim to analyse the interaction between the ambient environment and the ground temperature in the HGHE area. However, it also includes the influence of climatic conditions on the ground.

3. Results and Discussion

3.1. Basic Ground Heat Parameters

The heat parameters were measured in the ground with a Slinky-type HGHE in June 2012, during the exchanger stagnation period. The results are listed in Table 1.

Table 1. Basic thermal parameters of the ground.

| Depth (m) | t ($^{\circ}\text{C}$) | w (%) | λ (W/m·K) | C (MJ/m ³ ·K) | a (m ² /s) |
|-----------|----------------------------|---------|-------------------|----------------------------|-------------------------|
| 0.22 | 12.36 | 26.20 | 1.28 | 2.14 | 6.00×10^{-7} |
| 0.30 | 11.31 | 30.30 | 1.38 | 2.24 | 6.17×10^{-7} |
| 0.60 | 11.90 | 27.29 | 1.15 | 1.73 | 6.66×10^{-7} |
| 0.90 | 12.16 | 32.30 | 1.41 | 2.12 | 6.67×10^{-7} |
| 1.20 | 12.29 | 34.9 | 1.50 | 1.99 | 7.55×10^{-7} |
| 1.50 | 13.37 | 40.50 | 1.76 | 2.40 | 7.33×10^{-7} |
| 1.60 | 13.68 | 37.50 | 1.65 | 2.27 | 7.24×10^{-7} |

3.2. Ground Temperatures During the Heating Season

Table 2 summarizes the average daily temperatures of the ground with the linear HGHE and the parameters in Equation (1) for the heating season. The average daily temperatures during the heating season calculated from Equation (1) are plotted in Figure 5. The left vertical axis shows the temperatures t_{LR} of the ground with linear HGHE. The right vertical axis t_e shows the ambient temperature.

Both the data in Table 2 and the plot in Figure 5 demonstrate that the average daily temperature of the ground with the linear HGHE decreases toward the ground surface. The lowest temperatures were not attained in the HGHE; instead, they were observed near the mass surface. The oscillation amplitude Δt_A around the mean ground temperature \bar{t}_G increases toward the ground surface. Both trends confirm an appreciable effect of ambient temperature t_e . Some effect of the linear HGHE on the ground temperature is indicated by the difference between the mean ground temperature \bar{t}_G near the HGHE and the mean reference temperature t_{L11} , measured at a distance of 12.5 m from the HGHE centre, as well as by the difference between the oscillation amplitudes Δt_A in the ground with the HGHE and beyond it.

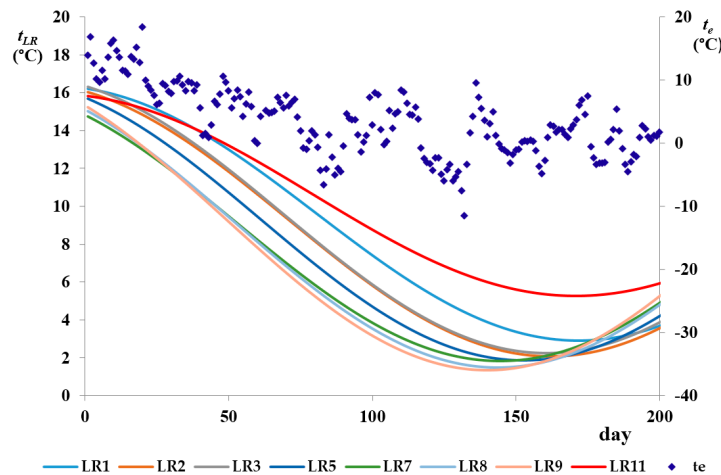


Figure 5. Plot of the average daily ground temperatures during the heating season—linear HGHE.

Table 2. Temperatures of the ground with the linear HGHE during the heating season and the appropriate parameters of Equation (1).

| Temp. (°C) | Average (°C) | Min. (°C) | Max. (°C) | Δt_A (K) | φ (rad) | \bar{t}_G (°C) | I_{yx}^2 (-) |
|------------|-----------------|-----------|-----------|------------------|-----------------|------------------|----------------|
| t_{LR1} | 8.04 ± 4.74 | 2.68 | 17.08 | 6.706 | 1.755 | 9.617 | 0.977 |
| t_{LR2} | 7.08 ± 4.76 | 2.00 | 17.14 | 7.207 | 1.922 | 9.290 | 0.978 |
| t_{LR3} | 7.23 ± 4.78 | 1.26 | 18.01 | 7.312 | 1.948 | 9.551 | 0.972 |
| t_{LR5} | 6.55 ± 4.57 | 1.61 | 17.43 | 7.429 | 2.085 | 9.290 | 0.950 |
| t_{LR7} | 6.06 ± 4.20 | 1.71 | 17.33 | 7.243 | 2.225 | 9.057 | 0.903 |
| t_{LR8} | 5.94 ± 4.39 | 0.66 | 17.32 | 7.627 | 2.238 | 9.126 | 0.904 |
| t_{LR9} | 5.86 ± 4.55 | 0.72 | 17.29 | 8.024 | 2.302 | 9.355 | 0.855 |
| t_{LR11} | 9.30 ± 3.74 | 5.23 | 16.74 | 5.337 | 1.772 | 10.591 | 0.984 |

Table 3 and Figure 6 show the average daily ground temperatures during the heating season for the setting with the Slinky-type HGHE and appropriate parameters in Equation (1). The left vertical axis shows the temperature t_{SR} of the ground with Slinky-type HGHE. The right vertical axis shows ambient temperature t_e .

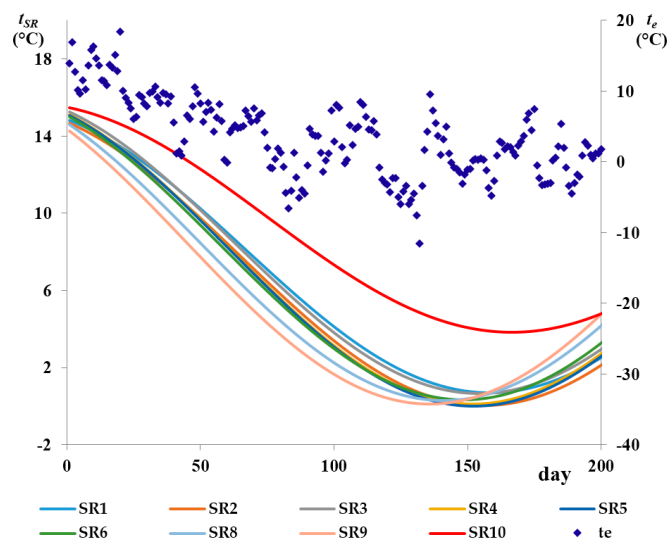


Figure 6. Plot of the average daily ground temperatures during the heating season—Slinky-type HGHE.

Table 3. Temperatures of the ground with the Slinky-type HGHE during the heating season and the appropriate parameters in Equation (1).

| Temp. (°C) | Average (°C) | Min. (°C) | Max. (°C) | Δt_A (K) | φ (rad) | \bar{t}_G (°C) | I_{yx}^2 (-) |
|------------|-----------------|-----------|-----------|------------------|-----------------|------------------|----------------|
| t_{SR1} | 5.64 ± 4.76 | 0.84 | 16.51 | 7.397 | 1.987 | 8.096 | 0.969 |
| t_{SR2} | 5.11 ± 4.94 | -0.19 | 16.54 | 7.736 | 2.022 | 7.783 | 0.946 |
| t_{SR3} | 5.64 ± 4.82 | 0.99 | 16.71 | 7.788 | 2.057 | 8.435 | 0.969 |
| t_{SR4} | 5.17 ± 4.92 | 0.36 | 17.08 | 8.095 | 2.096 | 8.187 | 0.961 |
| t_{SR5} | 5.10 ± 4.95 | 0.13 | 17.16 | 8.110 | 2.091 | 8.108 | 0.958 |
| t_{SR6} | 5.23 ± 4.75 | 0.60 | 17.03 | 8.034 | 2.154 | 8.374 | 0.949 |
| t_{SR8} | 4.96 ± 4.57 | 0.41 | 16.91 | 8.198 | 2.285 | 8.493 | 0.905 |
| t_{SR9} | 4.71 ± 4.51 | 0.31 | 16.80 | 8.421 | 2.376 | 8.531 | 0.804 |
| t_{SR10} | 8.16 ± 4.05 | 3.87 | 16.51 | 5.947 | 1.845 | 9.790 | 0.983 |

The decreasing trend of the average daily ground temperature and the increasing trend of oscillation amplitude Δt_A around the mean ground temperature \bar{t}_G in the setting with the Slinky-type HGHE are similar to those in the setting with the linear HGHE, although the former HGHE extracts heat from an appreciably smaller volume than the latter. The smaller mass volume is mirrored in the lower mean daily temperatures.

The determination index values I_{yx}^2 exhibit adequate precision of Equation (1), describing the ground temperature development during the heating season, for both HGHE types.

The decreasing trend of the average daily ground temperature and the increasing trend of oscillation amplitude Δt_A around the mean ground temperature \bar{t}_G in the setting with the Slinky-type HGHE are similar to those in the setting with the linear HGHE, although the former HGHE extracts heat from an appreciably smaller mass volume than the latter. The smaller mass volume is mirrored in the lower mean daily temperatures. The difference of the average daily ground temperature $t_{L1} - t_{S1}$ during the heating season, at a distance of 0.2 m below HGHEs was $\Delta t_1 = 2.28 \pm 1.13$ K. The ground temperature differences decrease toward the surface of ground. The difference of the average daily temperatures at a depth of 0.2 m below the surface was $\Delta t_9 = t_{L9} - t_{S9} = 1.13 \pm 0.71$ K.

The determination index values I_{yx}^2 exhibit adequate precision of Equation (1), describing the ground temperature development during the heating season, for both HGHE types.

3.3. Heat Flows and Specific Energies Extracted from the Ground

Figure 7 displays plot of the ground temperatures t_{L2} , t_{S2} in the HGHE area, the reference ground temperatures t_{L11} , t_{S10} beyond the HGHE area, and ambient temperatures t_e during the heating season. Furthermore, the plots in Figures 8 and 9 include the thermal output values $q_{s,L}$ and specific energies $q_{d,S}$, $q_{d,L}$ per m^2 of the HGHEs' external heat exchange area, and also the intensity $I_{s,r}$ and energy $I_{d,s,r}$ of the incident solar radiation during a day per m^2 . Specific thermal outputs q_L , q_S were determined based on the measured volume flow of heat transfer fluid, specific heat capacity and heat transfer fluid temperature difference at the inlet and outlet of the evaporator heat pump. Specific energies $q_{d,L}$, $q_{d,S}$ extracted from the ground were determined based on the specific thermal output and heat pump operation time at a certain power output. The results are summarised in Table 4.

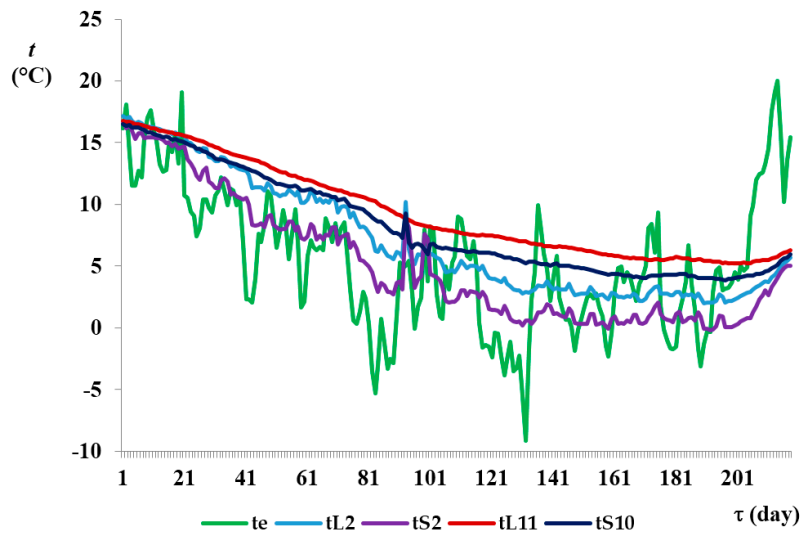


Figure 7. Ground temperatures in the HGHE area and ambient temperature during the heating season.

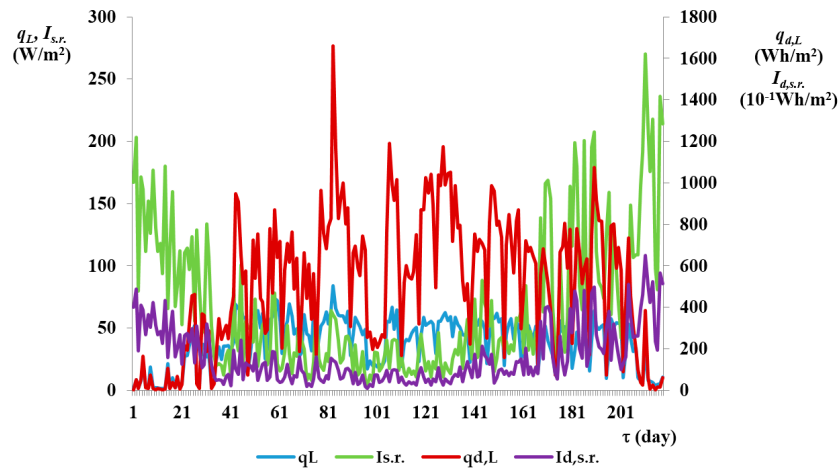


Figure 8. Development of the thermal outputs q_L , $I_{s,r}$ and energies $q_{d,L}$, $I_{d,s,r}$ during the heating season—linear HGHE.

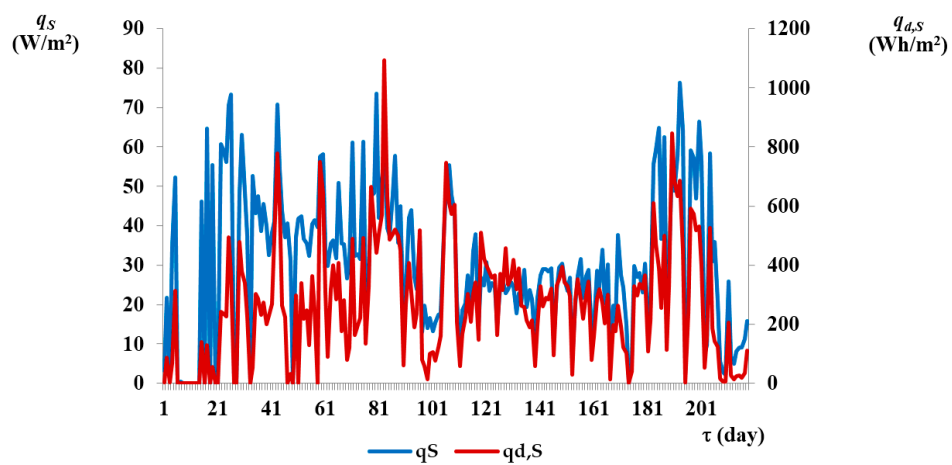


Figure 9. Development of the thermal outputs q_S and energies $q_{d,S}$ during the heating season—Slinky-type HGHE.

Table 4. Average and extreme values of the ambient temperatures, specific thermal outputs, and energies during the heating season.

| Physical Quantity | Min. | Average | Max. |
|---------------------------------------|-------|-------------------|--------|
| t_e (°C) | −9.15 | 5.44 ± 5.57 | 19.99 |
| q_L (W/m ²) | 1.36 | 38.49 ± 19.74 | 84.17 |
| q_S (W/m ²) | 0.00 | 30.08 ± 18.47 | 76.21 |
| $q_{d,L}$ (kWh/m ² ·day) | 2.22 | 0.51 ± 0.33 | 1.66 |
| $q_{d,S}$ (kWh/m ² ·day) | 0.00 | 0.27 ± 0.20 | 1.09 |
| $I_{s,r}$ (W/m ²) | 3.52 | 66.27 ± 55.35 | 270.29 |
| $I_{d,s,r}$ (kWh/m ² ·day) | 0.085 | 1.61 ± 1.35 | 6.49 |

The plots in Figure 7 and the summary data in Table 2 show that the average daily ground temperatures near the HGHEs were below zero. Minimum ground temperatures in the HGHE area were reached almost on the same days of the heating season. The minimum average daily temperature was $t_{L2} = 2.00$ °C (190 days) and $t_{S2} = -0.19$ °C (192 days) with linear HGHE and the Slinky-type HGHE, respectively. The temperatures were decreasing on average 1 K per 12.55 days and per 11.36 days with linear HGHE and Slinky-type HGHE, respectively. Due to the increasing ambient temperature at the end of the heating period, the average daily ground temperature in the HGHE area was also increasing. The ground temperatures t_{L2} , t_{S2} in the HGHE area at the end of the heating period differed by only 0.64 K and reached approximately 31.5% of the ground temperatures at the beginning of the heating season.

The average daily ground temperatures in the HGHE area were 1.97 ± 0.77 K higher for the linear HGHE than for the Slinky-type HGHE, while the total specific energy extracted from the HGHE during the heating season was nearly twice as high for the linear HGHE than for the Slinky-type HGHE. The ground temperatures in the HGHE area during the heating season were 68.8% (linear HGHE) and 53.6% (Slinky-type HGHE) higher than the ambient temperature t_e . VGHEs with a single U-tube exchanger (2 mm × 40 mm × 3.7 mm) and with a double U-tube exchanger (4 mm × 32 mm × 2.9 mm) were also examined at the same site, at the same ambient temperatures, and at the same heat-transfer fluid concentration. The average rock mass temperatures were lower for either of the VGHEs than for the linear HGHE. The rock mass temperatures in the VGHE area were higher than the ambient temperatures t_e only during 59.72% (single U exchanger) and 62.96% (double U exchanger) of the heating season.

The reference daily rock mass temperature t_{L11} measured 12.5 m from the centre of the linear HGHE heat exchange area was higher by an average 2.22 ± 1.23 K than the temperature t_{L2} within the linear HGHE area. The temperature t_{S10} measured 15.6 m from the centre of the Slinky-type HGHE heat exchange area was higher by an average 3.05 ± 1.41 K, compared to temperature t_{S2} .

The specific energies q_d extracted during a day of the heating season were 239.91 ± 198.35 Wh/m²·day in average higher with the linear HGHE than with the Slinky-type HGHE. The specific energies extracted from the ground over the entire heating season were 110.15 kWh/m² (linear HGHE) and 57.85 kWh/m² (Slinky-type HGHE). Additionally, the average specific thermal outputs q_L extracted from the ground by the linear HGHE were higher by 8.45 ± 16.57 W/m² than q_S extracted by the Slinky-type HGHE.

The better results obtained with the linear HGHE are presumably due to the larger mass volume from which the low-potential energy was extracted.

The importance of solar radiation for the ground energy potential can be documented by the total solar radiation energy hitting the ground surface during the heating season, which is $I_{\Sigma d,s,r} = 350$ kWh/m².

4. Conclusions

The operational testing of the HGHEs provided a deeper insight into the processes, usable in practical design and manufacturing work and, at the same time, inspiring future research trends in this field.

The monitoring and evaluation of the ground temperature changes during the heating season have shown that:

- The average daily ground temperature was primarily influenced by the ambient temperature t_e irrespective of the HGHE type. The average daily ground temperatures above the HGHEs during the heating season decreased toward the ground surface. Ground sensitivity to short-time ambient temperature changes has been noticed by Hepburn et al. [15], Popiel et al. [12], Inalli, Esen [5], and Zarrella and De Carli [17];
- The ground temperature near the HGHE was higher than ambient temperature t_e during 68.8% (linear HGHE) and 53.6% (Slinky-type HGHE) of the heating season. Ambient temperature was higher than the ground temperature particularly towards the end of the heating season. The importance of higher temperatures of a low-potential source for a heat pump has been pointed to by De Swardt, Meyer [11], as well as by Hepburn et al. [15];
- The average daily ground temperatures within the HGHE area were below zero only in the setting with the Slinky-type HGHE, and this was particularly toward the end of the heating season. Hypothesis *a*) formulated at the beginning of this paper was thereby confirmed;
- The average daily ground temperature within the HGHE area was 1.97 ± 0.77 K higher in the setting with the linear HGHE than in the setting with the Slinky-type HGHE. The minimum daily ground temperatures were also higher in the former setting than in the latter setting. Hypothesis *b*) was thereby confirmed;
- The reference average daily ground temperature beyond the HGHE area during the heating season was only 2.22 ± 1.23 K (linear HGHE) and 3.05 ± 1.41 K (Slinky-type HGHE) higher than that within the HGHE area. The differences between the reference ground temperatures and the temperatures within the HGHE areas are in accordance with the VDI recommendations [18];
- The average daily ground temperatures with the HGHEs during the heating season can be described by Equation (1) and by the parameters listed in Tables 2 and 3.

Measurements of the specific heat flows and the specific energies extracted from the ground during the heating season have shown that:

- The specific energies extracted from the ground during a day of the heating season q_d were higher by an average 239.91 ± 198.35 Wh/(m²·day) in the setting with the linear HGHE than in the setting with the Slinky-type HGHE. The specific energies extracted from the ground during the entire heating season were 110.15 kWh/m² for the linear HGHE and 57.85 kWh/m² for the Slinky-type HGHE. Hypothesis *c*) was thereby confirmed;
- The average specific thermal outputs q_L extracted from the ground by the HGHE were 8.45 ± 16.57 W/m² higher in the setting with the linear HGHE than in the setting with the Slinky-type HGHE. Hypothesis *c*) was thereby confirmed. Similar thermal output levels were reported by Wu et al. [20];
- Incident solar radiation plays an important role in the ground energy potential. The average incident solar radiation intensity during the heating season was $I_{s,r} = 66.27 \pm 55.35$ W/m². The total energies of solar radiation hitting the ground surface during the heating season were $I_{\Sigma d,s,r} = 350$ kWh/m². The data obtained by Hepburn et al. [15] and Wu et al. [19] were similar.

The measurements gave evidence that, with respect to the ground temperatures and energies extracted, the linear HGHE, as a low-potential energy source for heat pumps, is more convenient

than the Slinky-type HGHE. On the other hand, the former design requires a larger land area for its operation than the latter design.

Our forthcoming work will be aimed to optimise the HGHE configuration and GSHP operation with focus on a reduction of the land area required for energy extraction from the ground.

Author Contributions: All authors contribute equally to this paper.

Conflicts of Interest: The authors declare no conflict of interest.

Nomenclature

Abbreviations

| | |
|--------------|--|
| HGHE | Horizontal Ground Heat Exchanger |
| VGHE | Vertical Ground Heat Exchanger |
| GSHP | Ground Source Heat Pump |
| COP | coefficient of performance |
| EHPA | European Heat Pump Association |
| λ | thermal conductivity coefficient ($W/m \cdot K$) |
| C | specific heat capacity ($MJ/m^3 \cdot K$) |
| a | temperature conductivity coefficient (m^2/s) |
| t | temperature ($^{\circ}C$) |
| \bar{t} | mean temperature ($^{\circ}C$) |
| w | volumetric moisture (%) |
| Δt_A | oscillation amplitude around the temperature \bar{t} (K) |
| τ | number of days from the start of measurement (day) |
| φ | initial phase of oscillation (rad) |
| Ω | angular velocity ($2 \cdot \pi/365$ rad/day) |
| I_{yx}^2 | determination index (-) |
| $I_{s,r}$ | solar radiation intensity (W/m^2) |
| q | specific thermal output (W/m^2) |
| q_d | specific energy (Wh/m^2) |

Subscript

| | |
|-----|---------------------|
| L | linear HGHE |
| S | Slinky-type HGHE |
| e | ambient air |
| G | ground |
| R | regression function |
| d | day |

References

1. IPCC. Summary for Policy Makers, Climate Change 2014, Mitigation of Climate Change (2014). Available online: http://www.ipcc.ch/pdf/assessment-report/ar5/wg3/ipcc_wg3_ar5_summary-for-policymakers.pdf (accessed on 16 April 2016).
2. Residential Energy Consumption Survey (2014) EIA. Available online: <http://www.eia.gov/consumption/residential/> (accessed on 5 October 2015).
3. Aste, N.; Adhikari, R.S.; Manfren, M. Cost optimal analysis of heat pump technology adoption in residential reference buildings. *Renew. Energy* **2013**, *60*, 615–624. [[CrossRef](#)]
4. Nowak, T.; Jaganjacova, S. *European Heat Pump Market and Statistics Report 2013*, 1st ed.; European Heat Pump Association: Brussels, Belgium, 2014; p. 197.

5. Inalli, M.; Esen, H. Experimental thermal performance evaluation of a horizontal ground-source heat pump system. *Appl. Therm. Eng.* **2004**, *24*, 2219–2232. [[CrossRef](#)]
6. Neuberger, P.; Adamovsky, R.; Sed'ova, M. Temperatures and Heat Flows in a Soil Enclosing a Slinky Horizontal Heat Exchanger. *Energies* **2014**, *7*, 972–978. [[CrossRef](#)]
7. Adamovsky, D.; Neuberger, P.; Adamovsky, R. Changes in energy and temperature in the ground mass with horizontal heat exchangers—The energy source for heat pumps. *Energy Build.* **2015**, *92*, 107–115. [[CrossRef](#)]
8. Kupiec, K.; Larwa, B.; Gwadera, M. Heat transfer in horizontal ground heat exchangers. *Appl. Therm. Eng.* **2015**, *75*, 270–276. [[CrossRef](#)]
9. Brandl, H. Energy foundations and other thermal-active ground structures. *Géotechnique* **2006**, *56*, 81–122. [[CrossRef](#)]
10. Petit, P.J.; Meyer, J.P. Techno-economic analysis between the performances of heat source air conditioners in South Africa. *Energy Convers. Manag.* **1998**, *39*, 661–669. [[CrossRef](#)]
11. De Swardt, C.A.; Meyer, J.P. A performance comparison between an air-coupled and a ground-coupled reversible heat pump. *Int. J. Energy Res.* **2001**, *25*, 810–899. [[CrossRef](#)]
12. Popiel, C.; Wojtkowiak, J.; Biernacka, B. Measurements of temperature distribution in ground. *Exp. Therm. Fluid Sci.* **2001**, *25*, 301–309. [[CrossRef](#)]
13. Wu, Y.; Gan, G.; Verhoef, A.; Vidale, P.L.; Gonzalez, R.G. Experimental measurement and numerical simulation of horizontal-coupled slinky ground source heat exchangers. *Appl. Therm. Eng.* **2010**, *30*, 2574–2583. [[CrossRef](#)]
14. Gonzalez, R.G.; Verhoef, A.; Vidale, P.L.; Main, B.; Gan, G.; Wu, Y. Interactions between the physical soil environment and a horizontal groundcoupled heat pump, for a domestic site in the UK. *Renew. Energy* **2012**, *44*, 141–153. [[CrossRef](#)]
15. Hepburn, B.D.P.; Sedighia, M.; Thomas, H.R.; Manju. Field-scale monitoring of a horizontal ground source heat system. *Geothermics* **2016**, *61*, 86–103. [[CrossRef](#)]
16. Sanaye, S.; Niroomand, B. Horizontal ground coupled heat pump: Thermal-economic modeling and optimization. *Energy Convers. Manag.* **2010**, *51*, 2600–2612. [[CrossRef](#)]
17. Zarrella, A.; de Carli, M. Heat transfer analysis of short helical borehole heat exchangers. *Appl. Energy* **2013**, *102*, 1477–1491. [[CrossRef](#)]
18. VDI 4640–2:09–2001. *Thermal Use of the Underground—Ground Source Heat Pump Systems*; Verein Deutscher Ingenieure: Düsseldorf, Germany, 2001; p. 43.
19. Leong, W.H.; Tarnawski, V.R.; Aittomaki, A. Effect of soil type and moisture content on ground heat pump performance. *Int. J. Refrig.* **1998**, *21*, 595–606. [[CrossRef](#)]
20. Wu, W.; Wang, B.; You, T.; Shi, W.; Li, X. A potential solution for thermal imbalance of ground source heat pump systems in cold regions: Ground source absorption heat pump. *Renew. Energy* **2013**, *59*, 39–48. [[CrossRef](#)]
21. Song, Y.; Yao, Y.; Na, W. Impacts of Soil and Pipe Thermal Conductivity on Performance of Horizontal Pipe in a Ground-source Heat Pump. In Proceedings of the Sixth International Conference for Enhanced Building Operations, Shenzhen, China, 6–9 November 2006.
22. Banks, D. *An Introduction to Thermogeology: Ground Source Heating and Cooling*, 2nd ed.; John Wiley & Sons: Chichester, West Sussex, UK, 2012; pp. 332–344.
23. Go, G.H.; Lee, S.R.; Nikhil, N.V.; Yoon, S. A new performance evaluation algorithm for horizontal GCHPs (ground coupled heat pump systems) that considers rainfall infiltration. *Energy* **2015**, *83*, 766–777. [[CrossRef](#)]
24. IUSS Working Group WRB, 2006. *World Reference Base for Soil Resources 2006, A Framework for International Classification, Correlation and Communication (World Soil Resources Reports No. 103. FAO)*, 1st ed.; FAO: Rome, Italy, 2006; p. 143. Available online: <ftp://ftp.fao.org/agl/agll/docs/wsrr103e.pdf> (accessed on 16 April 2016).
25. Beer, F.P.; Johnston, E.R., Jr. *Vector Mechanics for Engineers: Statics and Dynamics*, 5th ed.; McGraw-Hill: New York, NY, USA, 1988; pp. 943–946.
26. Bowerman, B.L.; O'Connell, R.T. *Applied Statistics: Improving Business Processes*, 1st ed.; Richard D. Irvin Inc.: Boston, MA, USA, 1997; pp. 712–723.

